Full Papers
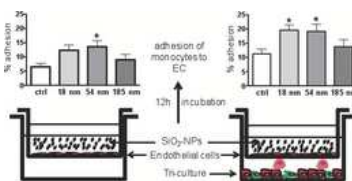
Endothelial Cells

D. Napierska, R. Quarck, L. C. J. Thomassen, D. Lison, J. A. Martens, M. Delcroix, B. Nemery, P. H. Hoet∗ ....x–xx
Amorphous Silica Nanoparticles Promote Monocyte Adhesion to Human Endothelial Cells: Size-Dependent Effect

The effect of amorphous silica nanoparticles (SiO₂-NPs) of different sizes on endothelial cells function is examined in vitro. Human endothelial cells are incubated with SiO₂-NPs in the presence or not of triple cell co-cultures. The results show that SiO₂-NPs enhance the adhesive properties of endothelial cells. This process is modified by the size of the nanoparticle and the presence of other co-cultured cells.

Author Proof

NANO | MICRO

small

Amorphous Silica Nanoparticles Promote Monocyte Adhesion to Human Endothelial Cells: Size-Dependent Effect

Dorota Napierska, Rozenn Quarck, Leen C. J. Thomassen, Dominique Lison, Johan A. Martens, Marion Delcroix, Benoit Nemery, and Peter H. Hoet*

ABSTRACT: There is evidence that nanoparticles can induce endothelial dysfunction. Here, the effect of monodisperse amorphous silica nanoparticles (SiO_2-NPs) of different diameters on endothelial cells function is examined. Human endothelial cell line (EA.hy926) or primary human pulmonary artery endothelial cells (hPAEC) are seeded in inserts introduced or not above triple cell co-cultures (pneumocytes, macrophages, and mast cells). Endothelial cells are incubated with SiO_2-NPs at non-cytotoxic concentrations for 12 h. A significant increase (up to 2-fold) in human monocytes adhesion to endothelial cells is observed for 18 and 54 nm particles. Exposure to SiO_2-NPs induces protein expression of adhesion molecules (ICAM-1 and VCAM-1) as well as significant up-regulation in mRNA expression of ICAM-1 in both endothelial cell types. Experiments performed with fluorescent-labelled monodisperse amorphous SiO_2-NPs of similar size evidence nanoparticle uptake into the cytoplasm of endothelial cells. It is concluded that exposure of human endothelial cells to amorphous silica nanoparticles enhances their adhesive properties. This process is modified by the size of the nanoparticle and the presence of other co-cultured cells.

1. Introduction

Nanotechnology is a rapidly growing activity that has elicited much concern because of the lack of available safety data. Engineered nanoparticles (NPs) represent a broad class of small-scale (<100 nm) entities, manufactured to achieve unique mechanical, optical, electrical or magnetic properties.[1] The application of synthetic amorphous silica nanoparticles (SiO_2-NPs), which are easily produced at a relatively low cost, has received wide attention in a variety of industries. SiO_2-NPs are produced on an industrial scale as additives to cosmetics, drugs, printer toners, varnishes, food and other products. In addition, during the last decade, silica-based nanomaterials have been successfully developed as drug and protein delivery vectors,[2,3] gene transfection reagents,[4,5] cell markers,[6] and carriers of molecules.[7] Due to the huge potential of SiO_2-NPs and their increased usage, occupational and public exposure will dramatically increase in the future. We have recently published a review on the health effects of nanosilica highlighting the growing evidence on the toxicity of SiO_2-NPs, both crystalline and amorphous.[8] However, more research with standardized materials is clearly needed to enable comparison of experimental data for the different forms of nanosilica.

It is generally agreed that the same properties that make nanomaterials so attractive for technological developments and

Dr. D. Napierska, Prof. B. Nemery, Prof. P. H. Hoet, Department of Public Health, Center for Environment and Health, Katholieke Universiteit Leuven, Herestraat 49, 3000 Leuven, Belgium; E-mail: peter.hoet@med.kuleuven.be
Dr. R. Quarck, Prof. M. Delcroix, Laboratory of Pneumology, Pulmonary Circulation Unit, Katholieke Universiteit Leuven, Herestraat 49, 3000 Leuven, Belgium
Prof. J. A. Martens, Center for Surface Chemistry and Catalysis, Katholieke Universiteit Leuven, Kasteelpark Arenberg 23, 3001 Heverlee, Belgium
Dr. L. C. J. Thomassen, Lab4U, Katholieke Hogeschool Limburg, Agoralaan B bus 3, 3590 Diepenbeek, Belgium
Prof. D. Lison, Louvain Centre for Toxicology and Applied Pharmacology, Université Catholique de Louvain, Avenue E. Mounier, 53.02, 1200 Brussels, Belgium
**10.1002**/smll.201201033

Table 1. Characteristics of the silica nanoparticles. The average diameter was obtained from TEM measurements. BET and external surface area (SA) were calculated from nitrogen sorption isotherms.

	Average particle size ± standard deviation [nm]	BET SA [$m^2 g^{-1}$]	External SA α-s method [$m^2 g^{-1}$][b]	Zeta potential in KCl [mV]	Zeta potential in DMEM [mV]
S-18	18.2 ± 2.1	254	185	−18	−15
S-54	53.8 ± 4.7	85	54	−67	−18
S-185	185.4 ± 22	12	9	−23	−16
FS-13	12.6 ± 1.4	258	199	−3	−4
FS-50	50.3 ± 4.8	77	67	−11	−17
FS-229	229 ± 19.6[a]	17	17	−16	−15

[a] Size of fluorescent core-shell particles. The sample also contained non fluorescent silica particles due to secondary nucleation; [b] Used for calculation of SiO_2-NPs concentration used in experiments.
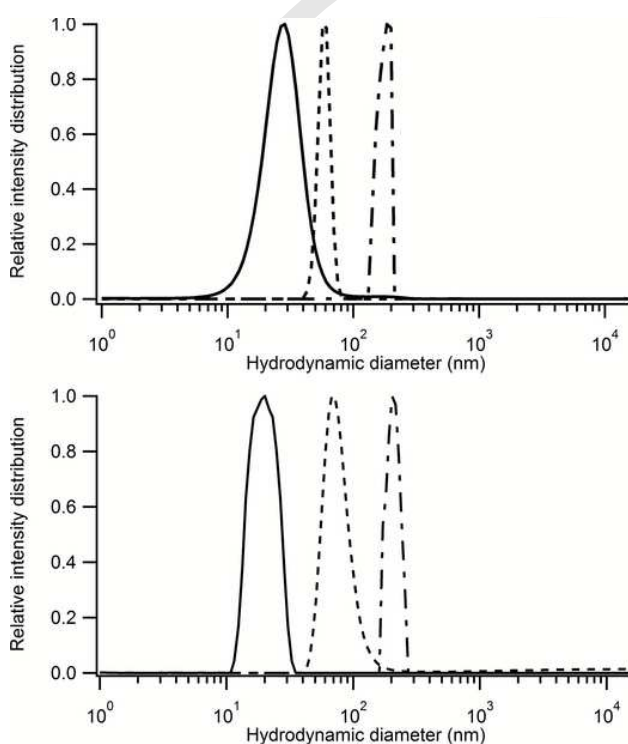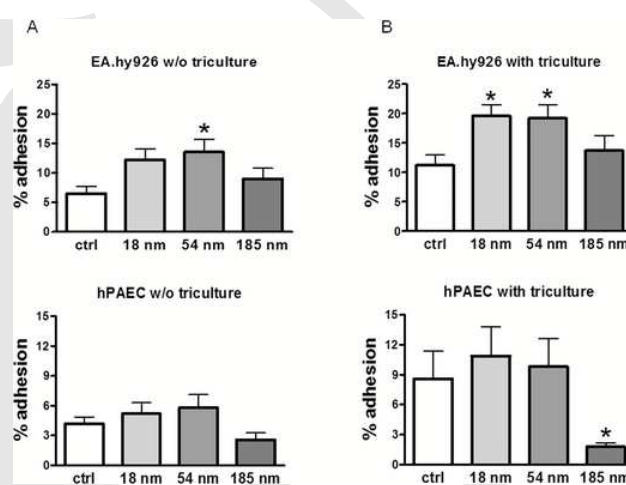

Figure 2. Hydrodynamic particle size distribution after 24 h in DMEM medium according to DLS. Upper panel A: S-18 (full line), S-54 (stripes), S-185 (dot-stipe); lower panel: FS-13: (full line), FS-50 (stripes), FS-229 (dot-stripe).

Figure 3. SiO_2-NPs-induced monocyte adhesion to endothelial cells. EA.hy926 and hPAEC cells were grown on Transwell inserts (nominal pore size of 0.4 μm) and exposed for 12 h to SiO_2-NPs (18, 54 and 185 nm). The cells were exposed to nanoparticles at concentration of 20 cm^2 SA (EA.hy926) and 10 cm^2 SA (hPAEC) per cm^2 of cell culture area surface; in the absence (A) or presence (B) of a human airway model consisting of a triple cell co-culture (B). After exposure, the cells were rinsed and monocyte adhesion test was performed as described in the Experimental Section.

cle surface. The specific surface areas estimated from the two approaches were in reasonable agreement (Table 1).

All dispersions of amorphous silica nanoparticles used in the study showed no detectable endotoxin contamination.

2.2. Effect of SiO₂-NPs on Human Monocyte Adhesion to Endothelial Cells

Incubation of EA.hy926 and hPAEC for 12 h with SiO_2-NPs (18, 54 and 185 nm), in the presence of a human airway model consisting of triple cell co-cultures, enhanced monocyte adhesion (**Figure 3**, panel B). The increase in adhesion (up to 2-fold) was

significant when EA.hy926 cells were incubated with 18 and 54 nm nanoparticles. In hPAEC cells, a similar trend was observed; however, due to higher inter-experimental variability, the differences between control and treated cells were not significant. The monocyte adhesion to hPAEC cells treated with 185 nm SiO_2-NPs was significantly lower compared to control. In contrast, exposure of both EA.hy926 and hPAEC cells to SiO_2-NPs in the absence of triple cell co-cultures in the basolateral compartment of the system, resulted in less pronounced adhesion of monocytes to EC (Figure 3, panel A). Endothelial cells viability was carefully checked at the end of each experiment; in all conditions, viability was consistently found to be higher than 90% compared to control.
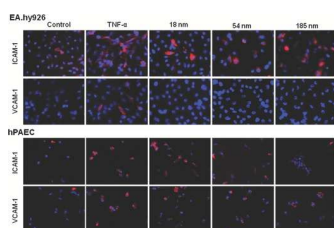
Figure 4. Expression of adhesion molecules in endothelial cells exposed to SiO$_2$-NPs. EA.hy926 and hPAEC cells were grown to a sub-confluent monolayer on glass culture slides and exposed for 12 h to TNF-α (10 ng mL^{-1}; positive control) and SiO$_2$-NPs (18, 54 and 185 nm). The cells were exposed to nanoparticles at concentration of 20 cm^2 SA (EA.hy926) and 10 cm^2 SA (hPAEC) per cm^2 of cell culture area surface. After exposure, the cells were fixed, permeabilized, and stained for ICAM-1 and VCAM-1 (red). Nuclei were stained with DAPI (blue).

2.3. Effect of SiO$_2$-NPs on EC Adhesion Molecules Expression

Incubation of human vein and primary human pulmonary artery endothelial cells for 12 h with SiO$_2$-NPs (18, 54 and 185 nm) induced expression of ICAM-1 but no VCAM-1 at EA.hy926 cell surface, and ICAM-1 and VCAM-1 at hPAEC surface (**Figure 4**). Real-time PCR measurements revealed significantly higher ICAM-1 mRNA expression in EA.hy926 cells after 6 h treatment with 18 nm nanoparticles (∼10-fold increase), and in hPAEC cells after 6 h treatment with 18 and 54 nm nanosilica particles (∼15-fold increase); no significant mRNA up-regulation was seen in the presence of 185 nm particles in endothelial cells (**Figure 5**).

2.4. Uptake of SiO$_2$-NPs in Endothelial Cells

The experiments performed with fluorescein FITC-doped SiO$_2$-NPs of 13, 50 and 229 nm showed internalization of all nanoparticles in both EA.hy926 and hPAEC (**Figure 6**). Confocal fluorescence microscope images indicated that SiO$_2$-NPs cumulated exclusively in cytoplasm and did not enter the nucleus of the exposed cells within the time window (12 h) of these experiments. The images of a z-stack show that some FS-229 particles formed big aggregates on the outer part of the cellular membrane (Figure S2 in SI).

Figure 5. SiO$_2$-NPs upregulated ICAM-1 mRNA expression in endothelial cells. EA.hy926 (A) and hPAEC (B) cells were grown to a sub-confluent monolayer in 6-well plate and exposed for 6h to TNF-α (10 ng mL^{-1}; positive control) and SiO$_2$-NPs (18, 54 and 185 nm). The cells were exposed to nanoparticles for 6 h at concentration of 20 cm^2 SA (EA.hy926) and 10 cm^2 SA (hPAEC) per cm^2 of cell culture area surface. The relative gene expression was determined by the comparative cycle threshold method ($2^{-\Delta\Delta CT}$), with gene of interest normalized to GAPDH gene expression. Results are reported as fold change over control (untreated cells) and expressed as the mean ± SD of two independent experiments performed in triplicates; ∗$p < 0.05$ and ∗∗$p < 0.01$ vs. control.

3. Discussion

Our experimental results show that exposure of human endothelial cells to monodisperse pure amorphous spherical silica nanoparticles enhance the adhesive properties of endothelial cells. This process is modified by the size of the nanoparticle and the presence of other co-cultured cells.

Inflammation and increased adhesiveness of the endothelial layer are considered to be initiating event for the developme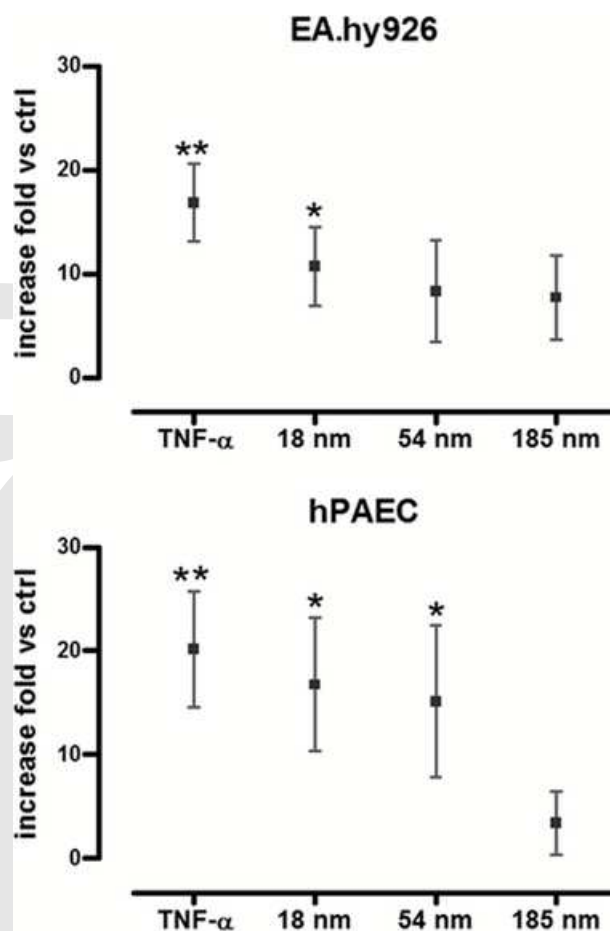nt of vascular diseases, such as atherosclerosis.[30] It has been shown that nanoparticles of different chemistry may play a role in exacerbating or accelerating this critical first step toward endothelial dysfunction. Gojova and co-workers reported that metal oxide nanoparticles (of different sizes; between 5 and 200 nm) can lead to dysfunction of the endothelium, but that this process was dependent upon particle composition.[31] Iron oxide, yttrium oxide and zinc oxide nanoparticles were all internalized into human aortic endothelial cells, but only yttrium oxide and zinc oxide were able to induce the expression of ICAM-1, interleukin-8, or CCL2 chemokine (monocyte chemo-
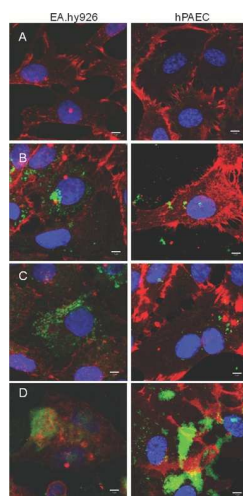
Size-Dependence of Monocyte Adhesion to Endothelial Cells with Silica

Figure 6. Confocal fluorescence images of endothelial cells after incubation for 12 h with SiO$_2$-NPs. The cells were exposed to nanoparticles at concentration of 20 cm^2 SA (EA.hy926) and 10 cm^2 SA (hPAEC) per cm^2 of cell culture area surface. (A) ctrl, (B) FS-13, (C) FS-50, (D) FS-229. Membranes were stained for CD31 (red). Nuclei were stained with DAPI (blue). Green colour indicates FITC-labelled nanoparticles. The size of the scale bar is 5 μm.

tactic protein-1) in aortic endothelial cells (HAECs). Oesterling et al.[32] demonstrated that alumina nanoparticles induced expression of endothelial cell adhesion molecules. Both porcine pulmonary artery EC and human umbilical vein EC showed increased mRNA and protein expression of VCAM-1, ICAM-1, and ELAM-1. Furthermore, human EC treated with alumina particles showed increased adhesion of activated monocytes.[32] The recent study indicates that silica NPs-induced activation and dysfunction of EC (HUVECs) is reflected by release of coagulatory protein von Willebrand factor and necrotic cell death.[33] Animal studies provide accumulating evidence that pulmonary inflammation caused by silica particles is accompanied by systemic endothelial cells dysfunction leading to enhanced blood coagulability by activation of clotting cascade.[34, 35]

Our previous study showed that exposure of human endothelial cells monoculture to monodisperse pure amorphous spherical silica nanoparticles caused cellular damage in a size- and dose-related manner.[36] We have also shown that these nanoparticles can up-regulate the in vitro secretion of cytokines (TNF-α, IL-6, IL-8 and MIP-1α) and that pro-inflammatory response in single cell cultures is amplified or mitigated in multiple co-cultures.[37] In this study, we report an increase in adhesive properties of endothelial cells in vitro, when exposed to amorphous monodisperse SiO$_2$-NPs. The increase in adhesion of monocytes observed in this study was significant when EA.hy926 cells were incubated with 18 and 54 nm nanoparticles. In hPAEC cells, a similar trend was observed. On the other hand, we found that protein expression of both ICAM-1 and VCAM-1 on the surface of hPAEC endothelial cells was up-regulated by all three nanoparticles. Real-time PCR measure-

ments revealed also significantly higher ICAM-1 mRNA expression in EA.hy926 cells after treatment with 18 nm nanoparticles, and in hPAEC cells after treatment with 18 and 54 nm nanosilica. ICAM-1 is a crucial mediator for the attraction and adhesion process of endothelial to leukocytes, and is involved in numerous lung diseases.[38, 39] The study with human dermal microvascular endothelial cells showed that moderately elevated ICAM-1 expression reduces endothelial cells barrier function (can cause leakiness), and that expressing higher levels of ICAM-1 affects cell junctions and the cytoskeleton.[40] Increased soluble ICAM-1 levels were found in the bronchoalveolar fluid and increased ICAM-1 expression was detected on alveolar macrophages and ATII cells of mice (adult female C57BL/6) instilled with crystalline silica particles.[41, 42]

The observed differences in the response to SiO$_2$-NPs between endothelial cells used in this study could result to some extent from obvious differences related to their nature: cell line vs. primary cells, different embryonic origin, different sensitivity, etc. Moreover, the observed differences in the cellular response to SiO$_2$-NPs between endothelial cell line and primary cells could also result, at least partially, from the presence of proteins in the incubation medium. While EA.hy926 cells were incubated with SiO$_2$-NPs in serum-free medium, exposure of hPAEC cells was performed in medium supplemented with 0.2% FCS and appearance of small agglomerates/aggregates was observed for S-18 and S-54. The concept of the nanoparticle-protein corona suggests that the adsorbed protein layer is an evolving collection of proteins that associate with NPs in biological fluids, influence their uptake and interaction with and within cells.[43, 44] Peetla and Labhasetwar were studying nanoparticle-endothelial model cell membrane interactions by measuring changes in the membrane's surface pressure (SP) during the interactions with NPs.[45] While aminated NPs (60 nm) increased SP, plain NPs reduced it, and carboxylated NPs of the same size had no effect. However, smaller NPs (20 nm) increased SP irrespective of surface chemistry, and serum did not influence their SP effect. Cell membranes are somewhat permeable and allow only small molecules to pass through. Uptake of nutrients and all communication among or between the cells and their microenvironment occurs through the plasma membrane by diverse mechanisms. Nevertheless, the proposed mechanisms of cellular uptake for NPs studied in different laboratories are inconsistent or even totally conflicting; there is an obvious need for a systematic understanding of the uptake and trafficking processes of NPs. Here, the uptake was studied in the serum-free medium (EA.hy926 cells) and medium supplemented with 0.2% fetal calf serum (hPAEC). We observed the uptake of SiO$_2$-NPs of all three sizes, and in both endothelial cells tested; this uptake was seen in the cytoplasm only. Detailed intracellular localization was not the subject of this study; however, in the previous study, endothelial cells (EA.hy926) exposed to silica nanoparticles (16 and 60 nm) were examined by electron microscopy.[46] Both nanoparticles were evident in endocytic vacuoles and, more strikingly, free in the cytoplasm. Non-encapsulated nanoparticles have been also observed by Corbalan and co-workers in the cytosol of human endothelial cells (HUVECs) exposed to amorphous SiO$_2$-NPs

with diameter of 10 nm.[47] Therefore, direct binding to proteins, altered protein conformation, changed downstream cellular signaling pathways (owing to structural effects) through nanoparticle interaction may be at work to produce observed endothelial dysfunction.

The human endothelial cell line has been chosen for the experiments as the continuation of the studies performed earlier with the same cells.[36] As primary cells more closely resemble physiological conditions *in vivo*, we also used primary human pulmonary arterial endothelial cells to study the uptake and adhesive properties of endothelial cells. Therefore, our findings might suggest an important role for nanoparticles-endothelial cell interaction which could contribute to development of vascular diseases. Previous immunohistochemical analyses have evidenced the presence of ICAM-1 and VCAM-1 on the endothelium in experimental and human atherosclerotic lesions.[48] Our results are in line with recent data showing that silica nanoparticles (20 nm) could induce dysfunction of HUVECs and increase expression of ICAM-1, VCAM-1 and E-selectin.[49]

The relevance of using *in vitro* cell co-culture systems to study interactions between nanoparticles and cells has recently been demonstrated.[50,51] It has been shown that co-culture systems respond to particles in a more realistic scenario with higher sensitivity than monocultures.[52–54] Muller and co-workers reported different response after nanoparticle exposure between cell monocultures and advanced three-dimensional culture model.[55] Our results confirm these observations; the presence of a human airway model consisting of triple cell co-cultures, enhanced the response of endothelial cells to SiO$_2$-NPs and increased monocyte adhesion.

In an attempt to speculate on the mechanistic aspects behind the observed activation of endothelial cells after incubation with SiO$_2$-NPs we would suspect that the production of reactive oxygen species (ROS) and/or the activation of redox sensitive signalling pathways are most probably involved.[49] However, our previous experiments on the effects of pure amorphous monodisperse SiO$_2$-NPs on endothelial cells did not reveal significant increases in ROS production/oxidative stress generation.[46] Other signalling pathway options have not been investigated, however, a number of possibilities exist including, e.g. overproduction of ONOO$^-$[47] or perturbations in calcium homeostasis.[56] The precise mechanisms for the observed effects of SiO$_2$-NPs on the endothelial cells deserve further investigations.

As silica nanoparticles are promising delivery vehicles for drug targeting or gene therapy, our observations are relevant. The main requirement for any nanocarrier material is biocompatibility which means it can be injected intravenously without toxicity and side-effects including activation of leukocytes, platelets, coagulation.[57]

4. Conclusion

The present findings suggest that direct contact between silica nanoparticles and endothelial cells promotes the up-regulation of the endothelial adhesion molecules expression and the adhesion of monocytes to endothelial cells. These effects are especially severe for silica of 50 nm and smaller. Our results suggest that a model of multi cell type culture is a useful tool to investigate local and systemic effects of nanomaterials *in vitro*.

5. Experimental Section

Synthesis and Characterization of SiO$_2$-NPs: Amorphous silica nanoparticles with a particle diameter of 18, 54 and 185 nm (S-18, S-54 and S-185) were synthesized under sterile conditions according to the Stöber procedure,[28] as previously reported.[29] The chemicals used for the synthesis were: ethanol (EtOH absolute), ammonium hydroxide solution (NH$_4$OH 25%, (w/v)), tetraethylorthosilicate (TEOS, 98%, (w/v)). Pyrogen free water was was used in the synthesis and purification procedures in order to eliminate endotoxin contamination. The composition of the synthesis mixtures is given in Table S1 (see SI). TEOS was added drop wise to the other components of the solution under stirring at 400 rpm.

Additionally, fluorescein (FITC) doped amorphous silica nanoparticles with a diameter of 13, 50 and 229 nm were prepared (FS-13, FS-50 and FS-229). To obtain these samples, tetraethylortosilicate was co-polymerized with the APTS-FITC conjugate in ethanol with ammonia as catalyst. The covalent bonding was assumed to prevent dye leakage. Reactant concentrations are listed in Table S1 (see SI). The APTS-FITC conjugate was synthesized by a reaction of fluorescein isothiocyanate isomer I (FITC, Acros), with the coupling agent APTS (3-aminopropyltriethoxysilane 99%, Acros). The amine group of APTS reacted with the isothiocyanate group of the dye to form a stable thiourea linkage. A 23 fold excess of APTS over FITC was used (69 mg APTS was added to 5.25 mg of FITC and stirred in 1 mL of anhydrous ethanol under nitrogen purge at room temperature for 24 h).

In both synthesis procedures, the sols were stirred for 24 h at room temperature to complete nanoparticle formation. Finally, ethanol and ammonia were removed by dialysis against pyrogen free water following the previously described procedure.[29]

TEM micrographs were obtained on a Philips CM200 FEG instrument operated at 200 kV. Aqueous suspensions of the silica nanoparticles were spread on a copper grid and allowed to dry in air overnight prior to TEM analysis. From TEM images, the diameter of 100 nanoparticles was measured to calculate the average particle diameter and standard deviation. Dynamic light scattering (DLS) was performed in a BIC 90 Plus instrument (Brookhaven) equipped with 654 nm laser (15 mW) under a detection angle of 90°. The sample preparation and measurements were described in detail elsewhere.[58] Zeta potential measurements were performed on a BIC ZetaPALS (Brookhaven Instruments Corporation, USA) in DMEM with a high ionic strength (conductance ca. 17 S) and in 3 mM KCl which is convenient for zeta potential determination because of its optimal ionic strength (conductance ca. 1 S).

The specific surface area of the powder samples was determined using nitrogen adsorption at −196 °C. Powder sam-

Author Proof

ples were dried at 150 °C under nitrogen flow for 12 h with a SmartPrep programmable degas system (Micromeritics) and analyzed on a TriStar surface area and porosity analyzer (Micromeritics). The total specific surface area, external surface area and the micropore volume of SiO$_2$-NPs were determined as described previously.[29]

Endotoxin Determination in SiO$_2$-NP Dispersions: Endotoxin concentrations were determined using a quantitative chromogenic Limulus Amebocyte Lysate (LAL) test (Charles River Laboratories, Charleston, US) following the manufacturer's instructions (for more details see SI).

Cell Culture: The following human-derived cell lines were used: A549 (epithelial type II pneumocytes; ATCC, Manassas, VA, USA); THP-1 (a monocyte derived cell line; ATCC) differentiated into macrophage-like cells by overnight incubation with phorbol myristate acetate; U937 (monocytic cells; a gift from the laboratory of clinical immunology of Katholieke Universiteit, Leuven, Belgium); HMC-1 (mast cells; kindly provided by J.H. Butterfield, Mayo Clinic, Rochester, MN, USA), EA.hy926 (immortalized umbilical vein cell line established by Edgell *et al.*).[59] Primary human pulmonary arterial endothelial cells (hPAEC; Invitrogen) were also used. For more details about the cell culture media see SI.

Experimental Conditions and Exposure to SiO$_2$-NPs: A tri-culture model was prepared in 12-well plates (basolateral compartment of the system) as described previously.[50] Briefly, cells (A549, THP-1 and HMC-1) were seeded at a total density of 1.6 × 10^5 cells cm^{-2} at a ratio of respectively 10:2:1. Endothelial cells (EA.hy926 or hPAEC) were grown separately until confluence on polyester Corning Transwell inserts with a nominal pore size of 0.4 mm. The cell culture medium in tri-culture was changed for FCS-free medium 12 h before inserts containing endothelial cells were introduced in the system (apical compartment). In parallel, endothelial cells in inserts were introduced in 12-well plates without tri-culture (only medium was present in the wells). The experimental design is presented in Figure S1 in SI.

The human endothelial cells were incubated with amorphous monodisperse SiO$_2$-NPs of three different sizes (S-18, S-54 and S-185) for 12 h. The EA.hy926 cultures were exposed to concentration of 20 cm^2 of nanoparticle surface area (SA) per cm^2 of cell culture area surface, in FCS-free medium. The hPAEC cultures were exposed to concentration of 10 cm^2 SA cm^{-2} of cell culture area surface, in medium containing 0.2% FCS. Applied doses were non-cytotoxic towards tested endothelial cells; addition of 0.2% FCS to the cell culture medium of hPAEC cells was necessary to sustain cell viability during the duration of experiments. The final nanoparticle dispersions were prepared immediately before use by serial dilution of the stock suspension followed by intense vortexing. Controls were incubated in an equivalent volume of DMEM. At the end of the exposure period, the viability of the cells was monitored by measuring lactate dehydrogenase (LDH) activity in medium.[60]

Cell Adhesion Test: After 12-h incubation with SiO2-NPs or vehicle, inserts containing endothelial cells were transferred to a new 12-well plate and washed twice with phosphate-buffered saline (PBS). Adhesion of human monocytes to endothelial cells was performed as described elsewhere.[61] Briefly, human monocytic U937 cells in suspension were radio-labelled with 1 μCi [^{3}H]-thymidine 10^{-6} cells for 48 h and were added (5 × 10^5 cells per well) to the endothelial cell monolayer for 3h at 37 °C. Non-adherent cells were washed out. Radioactivity incorporation was quantified as previously described.[62] The results are expressed as the percentage of adherent monocytes to the endothelial monolayer.

Adhesion Molecule Expression at Endothelial Cell Surface: Human vein and primary human pulmonary artery endothelial cells were incubated for 12 h with 20 and 10 cm^2 SA cm^{-2} of SiO$_2$-NPs (S-18, S-54 and S-185), respectively. TNF-α (10 ng mL^{-1}) served as a positive control. Cells were washed with phosphate-buffered saline (PBS) and fixed with acetone for 5 min at room temperature. The cells were blocked for 1 h with 3% bovine serum albumin in PBS at room temperature (RT). Adhesion molecule expression was assessed by using antibodies against human ICAM-1 or VCAM-1 diluted (1:50) in the blocking solution for 2 h at RT. Fluorescence labelling was obtained using the secondary antibodies Alexa544 goat anti-mouse (1:2000 dilution) for 1 h at RT. Staining with 4′,6-diamidino-2-phenylindole (DAPI; 10 μM) was used to visualize nuclei. FluorSave Reagent was used as mounting medium and slides were analyzed using an inverted Olympus IX81 fluorescence microscope. Negative controls were performed for every set of experiments by omitting the primary antibodies from the procedure.

Real-Time PCR Analysis for ICAM-1 Gene Expression in Endothelial Cells: Human vein and primary human pulmonary artery endothelial cells were incubated for 6 h with 20 and 10 cm^2 SA cm^{-2} SiO$_2$-NPs (S-18, S-54 and S-185), respectively, or with TNF-α (10 ng mL^{-1}; positive control).

After the treatment, cells were rinsed quickly with PBS, lyzed and total RNA was extracted using RNeasy Mini kit. The complementary DNA was synthesized using Ready-To-Go You-Prime First-Strand Beads kit and Oligo(dT)$_{12-18}$ primer, according to the manufacturer's instructions. For details concerning PCR measurements see SI.

Cellular Uptake: Core-shell fluorescent nanoparticles with a diameter of 13, 50 and 229 nm (hence a size very similar to that of the non-fluorescent SiO$_2$-NPs) were used to study the uptake of amorphous SiO$_2$-NPs by EA.hy926 and hPAEC. Endothelial cells were grown to sub-confluency on gelatine-coated glass culture slides, and then incubated with fluorescent nanoparticles (at concentration of 20 and 10 cm^2 SA cm^{-2}, respectively) for 12 h. Cells were rinsed three times with PBS and fixed with 4% formaldehyde in PBS for 20 min at RT. The fixed cells were permeabilized with 0.2% Triton-X100 in PBS, and blocked for 1 h with 3% bovine serum albumin in PBS at RT. Endothelial cells were labeled using a monoclonal antibody against CD31 diluted in the blocking solution for 2 h (1:25 dilution) at RT. Fluorescence labelling was obtained using the secondary antibody Alexa544 goat anti-mouse at 1:2000 dilution for 1h at RT. Staining with 10 μM DAPI was used to visualize nuclei. FluorSave Reagent (Calbiochem) was used as mounting medium and slides were analyzed using an inverted confocal fluorescence microscope (Zeiss LSM 510 META Laser

Author Proof

Scanning Microscope; 63x oil objective). Negative controls were performed for every set of experiments by omitting the primary antibodies from the procedure.

Statistical Analysis: Values are expressed as mean from three independent experiments ± standard deviation (SD). Each experimental value was compared to the corresponding control value. Statistical analyses were performed by one-way analysis of variance followed by Dunnett post hoc test. Differences among means were considered significant with $*p<0.05$, and $**p<0.01$.

Supporting Information

Supporting Information is available from the Wiley Online Library or from the author.

Acknowledgements

[1]   G. Oberdörster, E. Oberdörster, J. Oberdörster, *Environ. Health Perspect.* **2005**, *113*, 823–839.

[2]   J. M. Rosenholm, A. Meinander, E. Peuhu, R. Niemi, J. E. Eriksson, C. Sahlgren, M. Linden, *ACS Nano.* **2009**, *3*, 197–206.

[3]   I. I. Slowing, B. G. Trewyn, V. S. Lin, *J. Am. Chem. Soc.* **2007**, *129*, 8845–8849.

[4]   D. R. Radu, C. Y. Lai, K. Jeftinija, E. W. Rowe, S. Jeftinija, V. S. Lin, *J. Am. Chem. Soc.* **2004**, *126*, 13216–13217.

[5]   I. I. Slowing, J. L. Vivero-Escoto, C. W. Wu, V. S. Lin, *Adv. Drug Deliv. Rev.* **2008**, *60*, 1278–1288.

[6]   Y. S. Lin, C. P. Tsai, H. Y. Huang, C. T. Kuo, Y. Hung, D. M. Huang, Y. C. Chen, C. Y. Mou, *Chem. Mater.* **2005**, *17*, 4570–4573.

[7]   C. Y. Lai, B. G. Trewyn, D. M. Jeftinija, K. Jeftinija, S. Xu, S. Jeftinija, V. S. Lin, *J. Am. Chem. Soc.* **2003**, *125*, 4451–4459.

[8]   D. Napierska, L. C. Thomassen, D. Lison, J. A. Martens, P. H. Hoet, *Part Fibre. Toxicol.* **2010**, *7*, 39.

[9]   H. S. Choi, Y. Ashitate, J. H. Lee, S. H. Kim, A. Matsui, N. Insin, M. G. Bawendi, M. Semmler-Behnke, J. V. Frangioni, A. Tsuda, *Nat. Biotechnol.* **2010**, *28*, 1300–1303.

[10]   M. Geiser, B. Rothen-Rutishauser, N. Kapp, S. Schurch, W. Kreyling, H. Schulz, M. Semmler, H. V. Im, J. Heyder, P. Gehr, *Environ. Health Perspect.* **2005**, *113*, 1555–1560.

[11]   A. Nemmar, P. H. Hoet, B. Nemery, *Environ. Health Perspect.* **2006**, *114*, A211–A212.

[12]   G. Xie, J. Sun, G. Zhong, L. Shi, D. Zhang, *Arch. Toxicol.* **2010**, *84*, 183–190.

[13]   H. Nabeshi, T. Yoshikawa, K. Matsuyama, Y. Nakazato, K. Matsuo, A. Arimori, M. Isobe, S. Tochigi, S. Kondoh, T. Hirai, T. Akase, T. Yamashita, K. Yamashita, T. Yoshida, K. Nagano, Y. Abe, Y. Yoshioka, H. Kamada, T. Imazawa, N. Itoh, S. Nakagawa, T. Mayumi, S. Tsunoda, Y. Tsutsumi, *Biomaterials* **2011**, *32*, 2713–2724.

[14]   X. Lu, Y. Tian, Q. Zhao, T. Jin, S. Xiao, X. Fan, *Nanotechnology* **2011**, *22*, 055101.

[15]   K. Yamashita, Y. Yoshioka, K. Higashisaka, K. Mimura, Y. Morishita, M. Nozaki, T. Yoshida, T. Ogura, H. Nabeshi, K. Nagano, Y. Abe, H. Kamada, Y. Monobe, T. Imazawa, H. Aoshima, K. Shishido, Y. Kawai, T. Mayumi, S. Tsunoda, N. Itoh, T. Yoshikawa, I. Yanagihara, S. Saito, Y. Tsutsumi, *Nat. Nanotechnol.* **2011**, *6*, 321–328.

[16]   J. Wu, C. Wang, J. Sun, Y. Xue, *ACS Nano* **2011**, *5*, 4476–4489.

[17]   T. Yoshida, Y. Yoshioka, M. Fujimura, K. Yamashita, K. Higashisaka, Y. Morishita, H. Kayamuro, H. Nabeshi, K. Nagano, Y. Abe, H. Kamada, S. Tsunoda, N. Itoh, T. Yoshikawa, Y. Tsutsumi, *Nanoscale Res. Lett.* **2011**, *6*, 195.

[18]   X. Huang, J. Zhuang, X. Teng, L. Li, D. Chen, X. Yan, F. Tang, *Biomaterials* **2010**, *31*, 6142–6153.

[19]   Y. Song, X. Li, L. Wang, Y. Rojanasakul, V. Castranova, H. Li, J. Ma, *Toxicol. Pathol.* **2011**, *39*, 841–849.

[20]   M. A. Gimbrone Jr., *Am. J. Pathol.* **1999**, *155*, 1–5.

[21]   R. D. Brook, S. Rajagopalan, C. A. Pope III, J. R. Brook, A. Bhatnagar, A. V. ez-Roux, F. Holguin, Y. Hong, R. V. Luepker, M. A. Mittleman, A. Peters, D. Siscovick, S. C. Smith Jr., L. Whitsel, J. D. Kaufman, *Circulation* **2010**, *121*, 2331–2378.

[22]   A. J. LeBlanc, A. M. Moseley, B. T. Chen, D. Frazer, V. Castranova, T. R. Nurkiewicz, *Cardiovasc. Toxicol.* **2010**, *10*, 27–36.

[23]   Z. Li, T. Hulderman, R. Salmen, R. Chapman, S. S. Leonard, S. H. Young, A. Shvedova, M. I. Luster, P. P. Simeonova, *Environ. Health Perspect.* **2007**, *115*, 377–382.

[24]   A. Nemmar, M. F. Hoylaerts, P. H. Hoet, D. Dinsdale, T. Smith, H. Xu, J. Vermylen, B. Nemery, *Am. J. Respir. Crit Care Med.* **2002**, *166*, 998–1004.

[25]   A. Nemmar, M. F. Hoylaerts, P. H. Hoet, B. Nemery, *Toxicol. Lett.* **2004**, *149*, 243–253.

[26]   J. Geys, A. Nemmar, E. Verbeken, E. Smolders, M. Ratoi, M. F. Hoylaerts, B. Nemery, P. H. Hoet, *Environ. Health Perspect.* **2008**, *116*, 1607–1613.

[27]   S. P. Hudson, R. F. Padera, R. Langer, D. S. Kohane, *Biomaterials* **2008**, *29*, 4045–4055.

[28]   W. Stöber, W. Fink, E. Bohn, *J. Colloid Interface Sci.* **1968**, *26*, 62–69.

[29]   L. C. Thomassen, A. Aerts, V. Rabolli, D. Lison, L. Gonzalez, M. Kirsch-Volders, D. Napierska, P. H. Hoet, C. E. Kirschhock, J. A. Martens, *Langmuir* **2010**, *26*, 328–335.

[30]   P. Libby, *Nature* **2002**, *420*, 868–874.

[31]   A. Gojova, B. Guo, R. S. Kota, J. C. Rutledge, I. M. Kennedy, A. I. Barakat, *Environ. Health Perspect.* **2007**, *115*, 403–409.

[32]   E. Oesterling, N. Chopra, V. Gavalas, X. Arzuaga, E. J. Lim, R. Sultana, D. A. Butterfield, L. Bachas, B. Hennig, *Toxicol. Lett.* **2008**, *178*, 160–166.

[33]   A. T. Bauer, E. A. Strozyk, C. Gorzelanny, C. Westerhausen, A. Desch, M. F. Schneider, S. W. Schneider, *Biomaterials* **2011**, *32*, 8385–8393.

[34]   A. Nemmar, P. H. Hoet, B. Vanquickenborne, D. Dinsdale, M. Thomeer, M. F. Hoylaerts, H. Vanbilloen, L. Mortelmans, B. Nemery, *Circulation* **2002**, *105*, 411–414.

[35]   A. Nemmar, B. Nemery, P. H. Hoet, R. N. Van, M. F. Hoylaerts, *Am. J. Respir. Crit Care Med.* **2005**, *171*, 872–879.

[36]   D. Napierska, L. C. Thomassen, V. Rabolli, D. Lison, L.

Q2